J Mater Sci (2015) 50:3189–3199
DOI 10.1007/s10853-015-8882-7

Composite films of nanofibrillated cellulose and *O*-acetyl galactoglucomannan (GGM) coated with succinic esters of GGM showing potential as barrier material in food packaging

Victor Kisonen · Kasinee Prakobna · Chunlin Xu · Arto Salminen · Kirsi S. Mikkonen · Dimitar Valtakari · Patrik Eklund · Jukka Seppälä · Maija Tenkanen · Stefan Willför

Received: 21 November 2014 / Accepted: 30 January 2015 / Published online: 10 February 2015

Abstract Nanofibrillated cellulose (NFC)-Norway spruce *O*-acetyl-galactoglucomannan (GGM) composite films were coated either with a novel succinic ester of GGM or with native GGM. NFC films were made for reference. The succinic ester of GGM was synthesised at low (GGM-Su1) and high (GGM-Su2) degree of substitution to obtain different level of water repellence. GGM and its succinic esters had good affinity with NFC substrate. This made it possible to implement the barrier functionality on the NFC network with the adequate mechanical properties. The coatings further enhanced the already excellent oxygen permeability properties, achieving 0.1 [$(cm^3\ \mu m)(m^2\ kPa\ d)$] as the lowest value with the NFC-GGM film double-coated with GGM-Su2. The films demonstrated pronounced stiffness by adding GGM to the NFC, as well as coating of GGM-Su2 on the NFC-GGM films at 0–90 % relative humidity. The films turned out to be impenetrable with grease even at high temperatures. NFC-GGM film with GGM-Su2 coating exhibited hydrophobic characteristics according to the water contact angle measurements. It was shown that adding 5.5 wt% of GGM to a NFC film and further 5.4 wt% of coating of GGM-Su or GGM on the film may highly enhance the feasibility of the biocomposites to be used for food packaging to replace typical oil-based non-biodegradable plastics currently used.

Graphical abstract

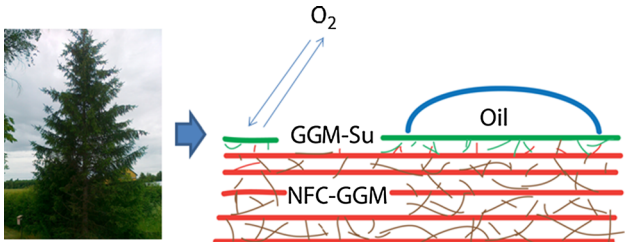

V. Kisonen (✉) · C. Xu · S. Willför
Laboratory of Wood and Paper Chemistry, Process Chemistry Centre, Åbo Akademi University, Turku, Finland
e-mail: vkisonen@abo.fi

C. Xu
e-mail: cxu@abo.fi

S. Willför
e-mail: swillfor@abo.fi

K. Prakobna · C. Xu
Wallenberg Wood Science Centre, KTH, Royal Institute of Technology, Stockholm, Sweden
e-mail: kasinee@kth.se

A. Salminen · J. Seppälä
Biotechnology and Chemical Technology, Polymer Technology, Aalto University, Espoo, Finland
e-mail: arto.salminen@aalto.fi

J. Seppälä
e-mail: jukka.seppala@aalto.fi

K. S. Mikkonen · M. Tenkanen
Department of Food and Environmental Sciences, University of Helsinki, Helsinki, Finland
e-mail: kirsi.s.mikkonen@helsinki.fi

M. Tenkanen
e-mail: maija.tenkanen@helsinki.fi

D. Valtakari
Laboratory of Paper Coating and Converting, Åbo Akademi University, Turku, Finland
e-mail: dimitar.valtakari@abo.fi

P. Eklund
Laboratory of Organic Chemistry, Åbo Akademi University, Turku, Finland
e-mail: peklund@abo.fi

Introduction

The petroleum-based packaging waste does not find its way only to landfills but also into seas, forests, and municipal landscapes. It degrades very slowly and pollutes the surrounding environment and is an extremely large hurdle all over the world. The small plastic particle waste (1–20 mm) is often dominant in the land areas next to the sea. These particles may place marine organisms at high risk due to possible ingestion [1]. Hence the appropriate legislation and attitude is needed to implement and promote the research, availability, and the production of biodegradable and bio-based materials. There is definitely an opportunity for the renewable natural fibres to be utilised as biomaterials. Thus, biopolymer composites are undoubtedly emerging [2].

Water soluble hemicelluloses can be obtained in large scale from side streams in mechanical pulping [3] or from pressurised hot-water extraction of wood [4–7]. Norway spruce *O*-acetyl-galactoglucomannan (GGM) is hydrophilic but it can be easily altered to more hydrophobic e.g. by grafting with non-polar groups [8] or by cross-linking chemically or enzymatically [9, 10]. Amphiphilic GGM derivatives have been made using fatty acids, cationic groups or hydrophobic tails of polydimethylsiloxane [11–13]. To make films solely of GGM, fairly high plasticiser content was required. The added glycerol in microfibrillated cellulose (MFC)-GGM films and decreased stiffness and strength but increased the elongation at break [14]. The incorporation of nanofibrillated cellulose (NFC) into pullulan films improved their mechanical properties. The addition of glycerol into these NFC-pullulan films enhanced the flexibility and homogeneity of the films and also increased the Young's modulus and tensile strength even up to 8000 % [15].

NFC has been used for packaging applications for its good mechanical properties and low gas permeability rates. Entangled networks with inter-fibrillary hydrogen bonding of nanofibres are known to improve mechanical properties [16, 17]. Yet, NFC has its drawbacks. It is hygroscopic and the mechanical properties are weakening upon wetting. Presumption is that NFC has good affinity to hydrophilic polymers, but not to hydrophobic polymers. Regardless, Okuba et al. demonstrated that MFC reinforced a polylactic acid–bamboo fibre matrix so that bending strength and fracture toughness improved and also crack growth was prevented [18]. To overcome the challenge of weak water repellence, the NFC was hydrophobised with silylation. The silylated material combined both hydrophobicity and oleophilicity and could selectively remove oil at the surface of water. At the oil–water interface, the cellulose nanofibrils were present as single dispersed fibrils or as a network [19, 20]. The fibre surface of NFC was hydrophobised by esterification with acetyl chlorides. A water dispersion of NFC was solvent-exchanged to acetone and then further with toluene [21]. NFC was incorporated into a matrix of acrylic polymer latex up to 15 wt% ratio, which led to major enhancement in the tensile modulus of the nanocomposite film [17]. The vulnerability of NFC composites towards the solvent has also been studied: NFC films had the ability to resist polar and nonpolar solvents, like methanol, and dimethylacetamide [22]. The films had been dried using elevated pressure in combination with heat and the resulted films could be soaked in both polar and nonpolar solvents for more than 18 h.

Functionality can be incorporated directly on the cellulose based on adhesion by hydrogen bonding and Van der Waals forces or by covalent bonding, for instance by using a linker [23]. Xyloglucan was used as a molecular anchor for setting up of polymers to cellulose surfaces. Xyloglucan oligosaccharides were incorporated into xyloglucan by enzymatic means to produce initiator-modified xyloglucan (XG-INI). Adsorption of XG-INI and subsequent atom transfer radical polymerization was utilised to alter cellulose surface properties and fabricate novel biocomposites. Furthermore, initiator introduction by adsorption did not harm the individual fibres or fibre structures. The reinforcing cellulose fibrils are embedded with cross-linked networks of hemicelluloses and lignin in wood cell wall. To mimic the plant cell wall structure, the composite films of NFC and GGM were prepared and an improved interaction between them was observed [24]. Thus, the composite films of NFC and GGM were used as substrates in the current study.

In food packaging several features can be tailored: for instance mechanical and optical properties, gas permeability and barrier properties, convenience in use, biodegradability, and the green image. Hemicelluloses are more favourable than cellulose fibrils for the chemical functionalization. Succinic ester of GGM with two different degrees of substitutions (DS) was synthesised to increase hydrophobicity. Hemicelluloses are known to have excellent oxygen barrier properties [25] and NFC is known to have excellent mechanical properties [26]. Hence, even with the added hydrophobic functionality within GGM based substrate can be well-established on the NFC network due to their chemical similarities. We aimed to enhance, grease- and oxygen barrier with GGM and GGM-Su coatings, the hydrophobicity with GGM-Su coatings and stiffness with GGM in the NFC network.

Materials and methods

Materials

The succinic anhydride was purchased from Fluka Ag. The benzoylated dialysis tube had a molecular weight cut-off of

2000 and was purchased from Sigma-Aldrich. Pyridin, DMF and D-sorbitiol were purchased from Sigma-Aldrich. The dispersion of NFC was prepared from softwood sulphite pulp (Nordic Pulp and Paper, Sweden) by subjecting to an enzymatic pretreatment according to Henriksson et al. [27].

GGM was obtained by pressurised hot-water extraction of Norway spruce wood [4]. The concentrate was further filtrated with a hydrophilic RC70PP regenerated cellulose acetate membrane (10 kDa, Alfa Laval) resulting in a GGM with M_w of 9 kg/mol [5]. A 17 % water dispersion of GGM was precipitated with 90 % ethanol followed by filtration and further washing with acetone and methyl *tert*-butyl ether.

Methods

Preparation of succinic ester of GGM

GGM (7.0 g, 15.9 mmol) was added to DMF (70 mL) and pyridine (14 mL) under magnetic stirring in a round-bottomed flask. The dispersion was heated to 80–85 °C (Succinic anhydride (7.5–18.6 g, 33–82 mmol and 0.8–2.0 eqv.) was then added to the dispersion and was kept under heating for 1.5 h. Eventually the dispersion was evaporated to small volume and was dissolved in 67 % (v/v) ethanol–water or in water and purified by dialysis against water.

Preparation of nanofibrillated cellulose

The pretreated pulp prepared by enzymatic treatment was disintegrated by passing through a microfluidizer (Microfluidics Ind., USA) connected to series of chambers with diameters of 400, 200 and 100 μm for several times [28]. The NFC dispersion was diluted with deionized (DI) water to obtain a final concentration of 0.2 wt% before film formation.

Preparation of NFC films

The diluted NFC dispersion was mixed at 8000 rpm using an Ultra Turrax mixer (IKA, T25 Digital). The NFC film was subsequently prepared by filtration on a fine membrane and dryid using Rapid Köthen Sheet Former, according to a previously reported method for the nanopaper [29].

Preparation of NFC-GGM composite film

Aqueous dispersion of 0.1 wt% GGM was prepared with de-ionised water. The GGM dispersion was heated shortly at 90 °C to improve solubility of GGM prior to mixing with the NFC dispersion. Moreover, the GGM dispersion was filtered through a fine nylon cloth in order to remove the water-insoluble fraction in advance. A thorough mixing was performed on the mixture of NFC and GGM dispersions at 90 °C for 4 h. The NFC-GGM film was further prepared by filtration and drying similarly to the NFC reference film. During filtration, a major portion of GGM was lost through the fine membrane. The GGM content was determined by weighing the left-over GGM. The NFC-GGM film with a final GGM content of 5.5 wt% was successfully prepared and selected for the further coating study.

Coating of the films

15 wt% water dispersion of GGM or GGM-Su1 or 15 wt% ethanol dispersion of GGM-Su2 with 15 wt% of sorbitol (relative to GGM) was prepared for the coating of the films. The coating was performed with a K-control (bar) coater. The wet coating was dried under UV lamp for ~6 s and then placed between two polyamide meshes with 36.5 μm pore size followed by two plotting papers and plastic boards with 4.5 kg weight on a top. The entity was put into a vacuum oven at 40 °C for the further 18 h.

Characterisation

Dynamic mechanical analysis (DMA) in humidity mode

Dynamic mechanical analysis (DMA) on NFC-GGM films was carried out with a Q800 dynamic mechanical analyzer (TA Instruments, USA). The analysis was performed in tensile mode using a controlled relative humidity (RH) accessory. The preload force, amplitude and frequency during the experiments were 0.05 N, 5.0 μm and 1 Hz, respectively. The sample dimensions were approximately $10.00 \times 5.30 \times 0.02$ mm^3. The storage moduli (E') of NFC-GGM films were recorded as a function of time at 30 °C. Samples were initially equilibrated at 0 % RH and 30 °C. The DMA scan was performed in a stepwise manner at RH values of 0, 50, 90 % and once again at 0 % to record the extent of material recovery. Each humidity level was sustained for 300 min. Three parallel specimens were measured from each sample to calculate the average storage modulus at different RH values after 300 min equilibration.

NMR

Nuclear magnetic resonance (NMR) spectra were recorded using Bruker advance NMR spectrometers operating at 600.13 MHz (150.90). The results are expressed in ppm scale. The samples were dissolved in DMSO-d_6 (170 mg/mL) and run at 40 °C; DMSO was used as the internal standard. A 15-s pulse delay (D1) and an inverse-gated

decoupling pulse sequence were used for quantitative ^{13}C measurements and 2 s pulse delay for qualitative ^{13}C measurements and 1.5 s pulse delay for HMBC measurements. About 15,000 scans were performed in ^{13}C NMR and 276 scans for HMBC.

Grease barrier properties

Food-grade rapeseed oil was applied on the films. 100 mL of oil was coloured with 1 g of 1-[[2-methyl-4-[(2-methylphenyl)azo]phenyl]azo]-2-naphthalenol (solvent red 24). Grease barrier properties were first tested with the traditional Tappi 454 method [30], but that method did not work due to the probable deposition of oil onto the surface of the film and consequent drying of the oil reservoir. We instead used a surplus of oil without the external pressure [31, 32]. The oil was put into the cylinder hole. Grease barrier was determined with a method of where cylinder on top of the film was filled with coloured rapeseed oil, and the sorption paper was underneath. The films had been conditioned for 24 h at 23 °C and at 50 % RH prior to testing.

Oxygen permeability

The oxygen gas transmission rate (OTR) of the films was measured using an oxygen permeability (OP) analyser with a coulometric sensor (M8001; Systech Illinois, Oxfordshire, UK). The film was exposed to 100 % oxygen on one side and to oxygen-free nitrogen on the other side for the overnight measurement. The OP was calculated by multiplying the OTR by the thickness of the film and dividing it by the oxygen gas partial pressure difference between the two sides of the film. The measurements were carried out at 23 °C, normal atmospheric pressure, and at 50 % RH. The specimen area was 5 cm^2 and the thickness of the film was measured before analysis at five points with a micrometer at 1 μm precision. The OP was determined in duplicates.

Scanning electron microscope

The cross-section surfaces and the surfaces of the films were viewed with scanning electron microscopy (SEM). The SEM was manufactured by LEO, Oberkochen, Germany. An UltraDry silicon drift detector was used. Rectangular strips of approximately 5 × 40 mm were put into liquid nitrogen and manually fractured using a razor blade. The fragments were mounted on aluminium stubs, using conductive carbon tape, and coated with a carbon evaporator by direct-current sputtering. The SEM was operated under high vacuum, using secondary electron-imaging mode. The magnification of the image corresponds to a Polaroid 545 print with the image size of 8.9 × 11.4 cm.

Water contact angle

Contact angle (CA) measurements were carried out with a KSV CAM 200 (later Biolin Scientific) optical goniometer and OneAttension Theta1.4 software. 18.2 MΩ type-1 (Milli-Q) DI distilled water was used. 3 μL drops were released onto the sample surface with the sessile drop measurement method. At least five different measurements per specimen were carried out. The measurements were finished at 550 s time.

Results and discussion

Succinylation of GGM

Succinic anhydride was used to prepare the novel GGM-Su1 (low DS) and GGM-Su2 (high DS) at 80–85 °C according to our previously reported method of esterification (Scheme 1) [8].

The DS of the succinic ester of GGM was obtained using quantitative ^{13}C NMR by quantifying the intensity ratio of the signal of two methylene carbons (Fig. 1: C8 and C9, $\delta = 31$ ppm,) against the C1 signal (Fig. 1) according to the equation: $\mathrm{DS} = \frac{0.5 \times C(\mathrm{meth})}{C(\mathrm{anom})}$, where C(meth) equals the quantity of signals of methylene carbons and C(anom) equals the quantity of the signal of the anomeric carbon. This is in line with the sum of signals of carbonyls of the succinic group, C7 and C10, also quantified against the signal of C1. The DS value of GGM-Su1 was 1.0 and 1.6 for GGM-Su2, respectively. Heteronuclear multiple bond correlation NMR (HMBC) reveals two or three bond correlation between proton and carbon. By HMBC we can point out the carbonyl of the acetyl group at $\delta = 171.5 \leftrightarrow 2.0$ ppm. As the C6 gets substituted by succinic group, the chemical shift moves to higher frequency (Fig. 1) [33, 34], which additionally points out the presence of the succinic substituent. The percentage of the total DS on C6 of GGM-Su1 and GGM-Su2 are 57 and 74 %, respectively.

Preparation of the composite films

The amount of GGM in the NFC films was optimised by absorption tests, resulting in 5.5 wt% of GGM in a film. The amount was in line with the mechanical properties. Also pristine NFC films were prepared for comparison. The coating was carried out with a bar coater resulting in 5.4 wt% increase, yielding translucent films (Fig. 2). The GGM-Su1, GGM-Su2 and GGM were applied on the NFC-GGM film and GGM-Su2 also on the NFC film resulting in 5.4 wt% increase. Ethanol was used as solvent for the

Scheme 1 Succination of GGM. *Py* pyridine, *DMF* dimethylformamide

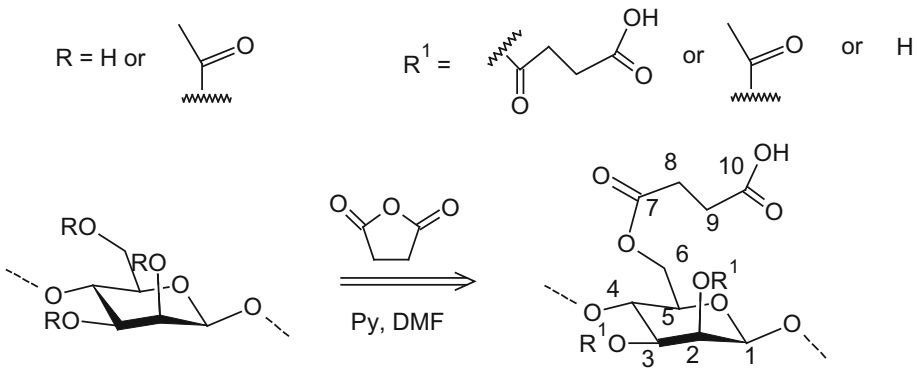

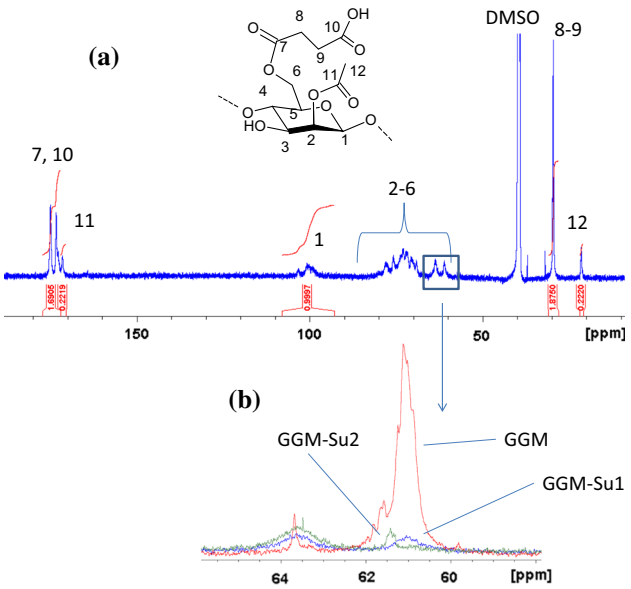

Fig. 1 The quantitative ^{13}C NMR of GGM-Su1 (**a**). C6 substitution pattern of the GGM and GGM-Su1 and GGM-Su2 with the quantitative C^{13} NMR (**b**). The signal of non-substituted C6 is at $\delta = 60.0$–62.1 ppm, while the signals of GGM-Su1 and GGM-Su2 have shifted to $\delta = 62.6$–65.4 ppm

coating GGM-Su2 (high DS), while water was used for the rest. Based on our previous studies, 15 wt% of sorbitol (relative to GGM) was added to the dispersions to render more coherent film-like structure and potentially better oxygen barrier properties (Fig. 2).

The film surface–water interaction

We observed wetting behaviour of the film surface with the sessile water drop CA determination method. According to the Young equation, $\gamma_{sv} = \gamma_{sl-}\gamma_{lv}\cos\theta_Y$, where γ_{sv}, γ_{sl} and γ_{lv} represent the solid–vapour, solid–liquid and liquid–vapour interfacial tensions, respectively, and θ_Y is the drop CA. Surfaces showing water CA $> 90°$ lean towards hydrophobic behaviour and CA $< 90°$ lean towards hydrophilic behaviour. The Young equation describes the wetting on ideal surfaces and does not consider the impact of surface topography [35]. However, when water drop volume and baseline (wetting diameter of the drop) information is used side-by-side with the CA, additional information about film heterogeneity or water absorption into the film can be unveiled. The representative individual cases are illustrated in the Figs. 3 and 4 and the average CA values at 1 s are given in Table 1.

Our results can be split into two categories based on the film wetting properties. In the first category, films produced solid, sloped straight line CAs and drop volumes complemented with flat baselines as a function of time. The baseline remained fairly constant i.e., there was no increase of the wetting area throughout the measurement. Hence, the change in CA over time was solely dependent on the evaporation of the drop. The pristine NFC and NFC-GGM films and NFC-GGM film coated with GGM-Su2 belong to this category. The NFC-GGM film coated with GGM-Su2 showed the highest CA (78°) of the three. Hydrophobic domains on the surface hinder water molecules from advancing [35]. Surprisingly GGM within the NFC film did increase the CA in comparison to the pristine NFC film. Spiridon et al. [36] suggest that addition of cellulose into starch based composite films improves their water resistance due to strengthened inter-component hydrogen bonding. The extensive hydrogen bonding between GGM and NFC may disfavour the hydrogen bonding sites for water molecules [37]. Acetyl groups of GGM makes GGM water soluble for spacing out the polymer chain, but upon incorporated onto the solid film matrix, they may increase the hydrophobicity.

In the second category for NFC-GGM coated with GGM or GGM-Su1. It took roughly 100 s for CA curve to straighten up. The baseline graph shows similar delayed increase of the wetting area. Both these films have lower initial CA (55° and 61° for GGM and GGM-Su1 coatings, respectively) than pristine NFC film (63°) or NFC-GGM composite film (76°), making them more hydrophilic than their counterparts in the first category. The advancement of

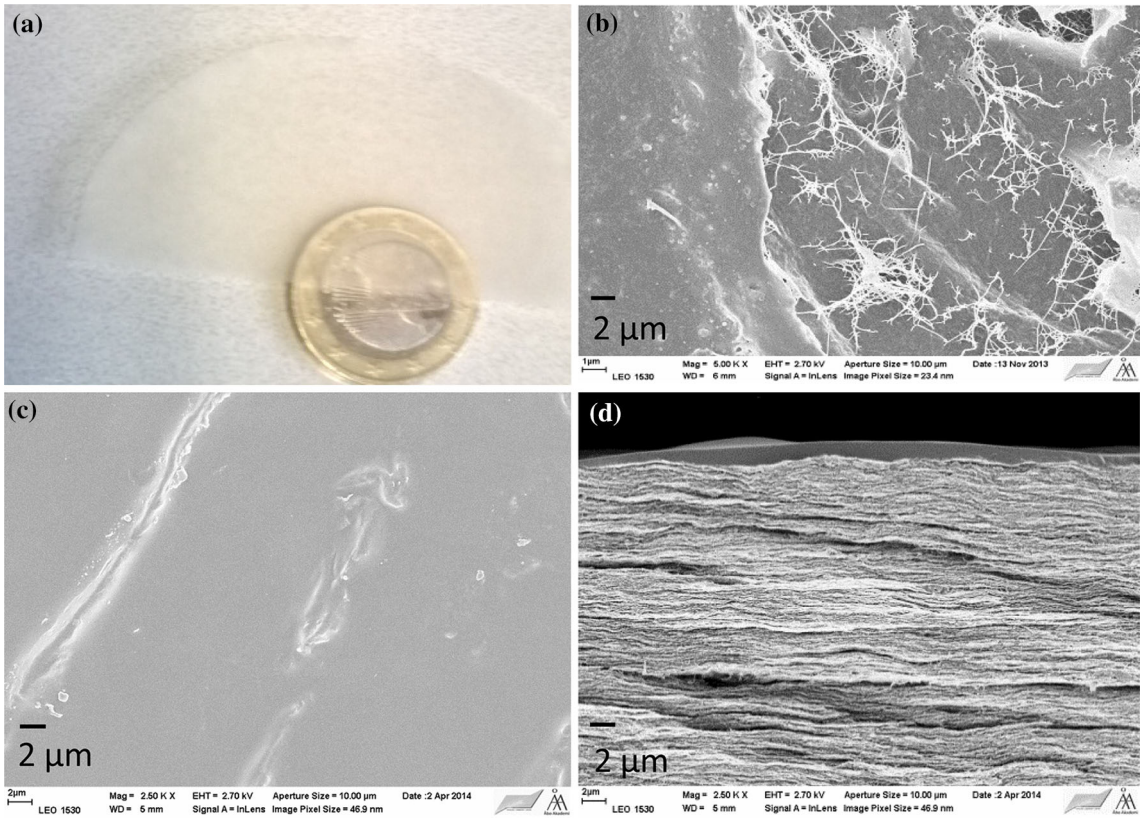

Fig. 2 Photo of translucent NFC-GGM film (**a**), SEM pictures of the NFC-GGM film (**b**), NFC-GGM film coated with GGM-Su1: a *top* (**c**) and of a cross-section (**d**) image

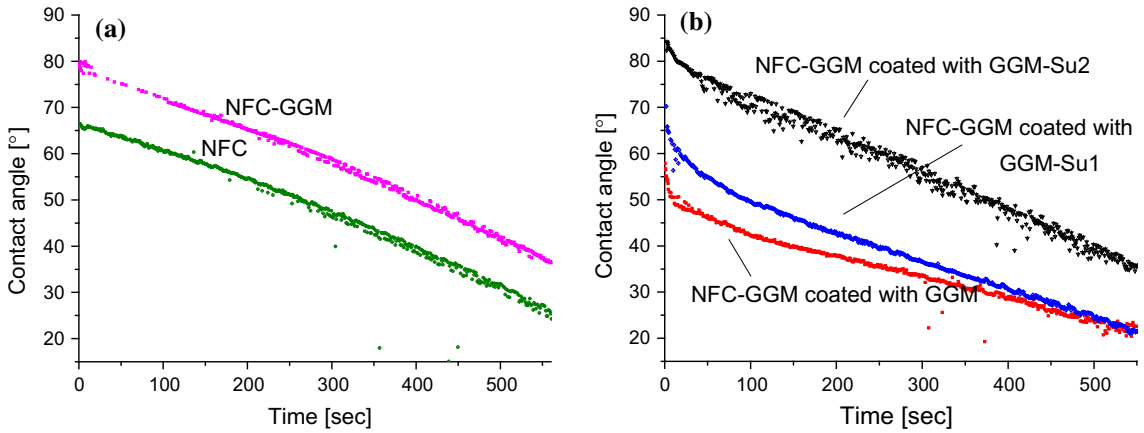

Fig. 3 The water contact angles as a function of time on NFC-GGM and NFC films (**a**) and NFC-GGM films coated with GGM-Su2, GGM-Su1 and GGM (**b**)

the CA went hand-in-hand with the non-linear increase of the baseline, which kept the drop volume constant over time—an indication of non-absorption of water into the film matrix. In the literature, GGM films have obtained the CA values of 63° [38], which is near to the value of our GGM coating on NFC-GGM film. Pristine NFC films had CA values of 40° but increased to 110° due to the wax treatment [22]. Yet, different ways of producing the NFC and different preparation technique make the direct comparison inadequate.

Grease barrier property

Grease barrier was determined with the method where a cylinder on top of the film was filled with surplus of

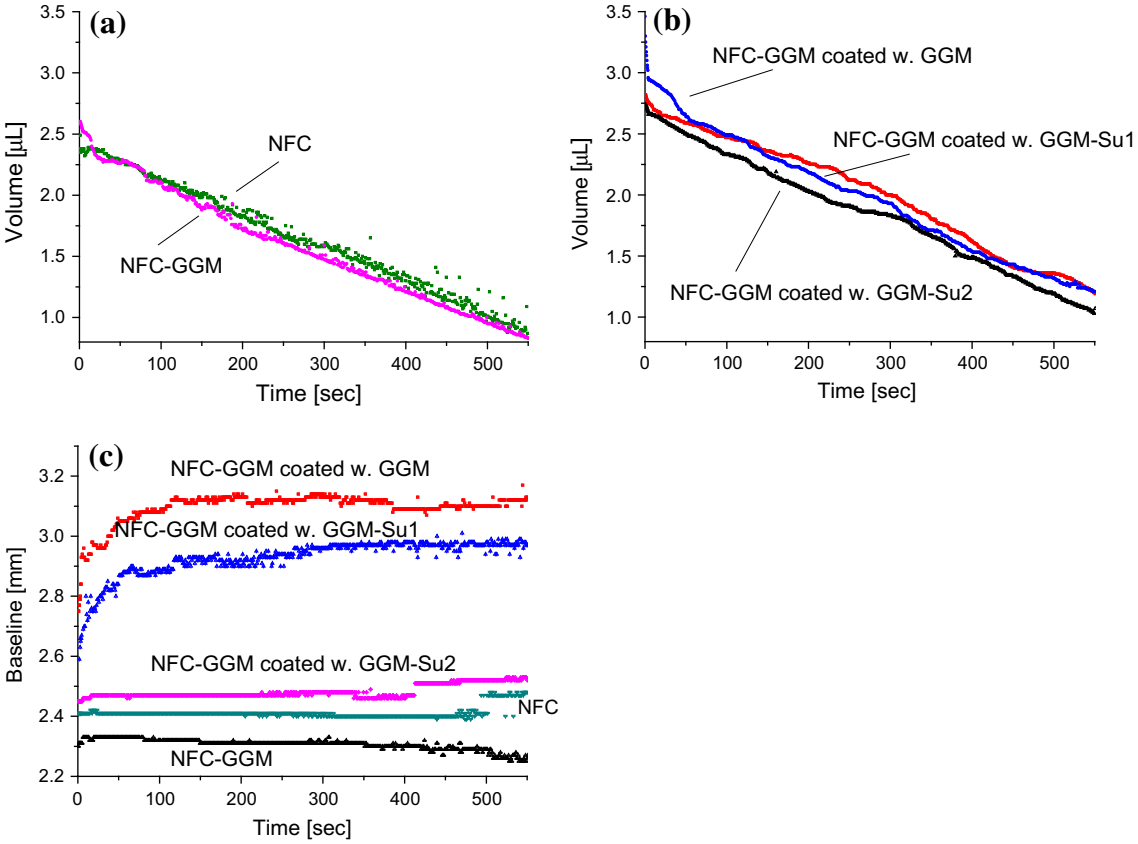

Fig. 4 The water drop volume (**a**, **b**) and baseline (**b**) as a function of time on a film surface

Table 1 The water contact angle value on the films at 1 s

The matrix	The coating	Water contact angle at 1 s (°)
NFC	–	63 ± 3
NFC	GGM-Su2	67 ± 6
NFC-GGM	–	76 ± 6
NFC-GGM	GGM	55 ± 1
NFC-GGM	GGM-Su1	61 ± 6
NFC-GGM	GGM-Su2	78 ± 5

coloured rapeseed oil. Biopolymer films have the tendency of poorer barrier and mechanical properties at elevated RH. We tested the grease barrier for rapeseed oil in exotic conditions, where the edges of the film were exposed to the high RH. No oil penetration was observed for NFC-GGM at 60 °C and at 75 % RH in 5-day-long tests. Both the pristine NFC films and the NFC-GGM composite films coated with NFC-GGM-Su1 were also impenetrable at 50 °C and at 50 % RH in 6-day-long tests. NFC-GGM composite film coated with GGM-Su2 was impermeable for 11 days at 50 °C and at 40 % RH followed by 9 months at 23 °C at 50 % RH. The SEM pictures show the possible oil deposition on a surface of the film (Fig. 5).

The results with chitosan coating for a greaseproof paper were comparative to the grease barrier of commercial poly(ethylene terephthalate) [39]. Arabinoxylan films provided 100 % barrier against sunflower oil for 48 h at 60 °C [40]. NFC films were grease proofed for the measured time of 4 h at 60 °C [22]. Thin layer (1 g/m^2) of benzoyl and phthaloyl ester of GGM on cartonboard made about 50 h barrier for grease at ambient temperature [41].

Oxygen barrier property

The OP and oxygen transmission (OT) was determined from two replicates at 23 °C and at 50 % RH and the values are shown in Table 2.

GGM coating and GGM-Su2 double-coating decreased the OTR value of NFC-GGM film from 3.2 to 1.1 and 0.2 cm^3/(m^2 d) respectively. The partial pressure and the film thickness differences were considered in the OP test, unlike in the OTR test. Upon comparison of the OP to the OTR values, where the differences were larger but the trend resembled that of the OP values. The NFC film had an OP value of 0.5 [(cm^3 µm)(m^2 kPa d)] and NFC-GGM of 0.9 [(cm^3 µm)(m^2 kPa d)]. Integration of GGM made may have led to less dense NFC reinforced network. GGM-

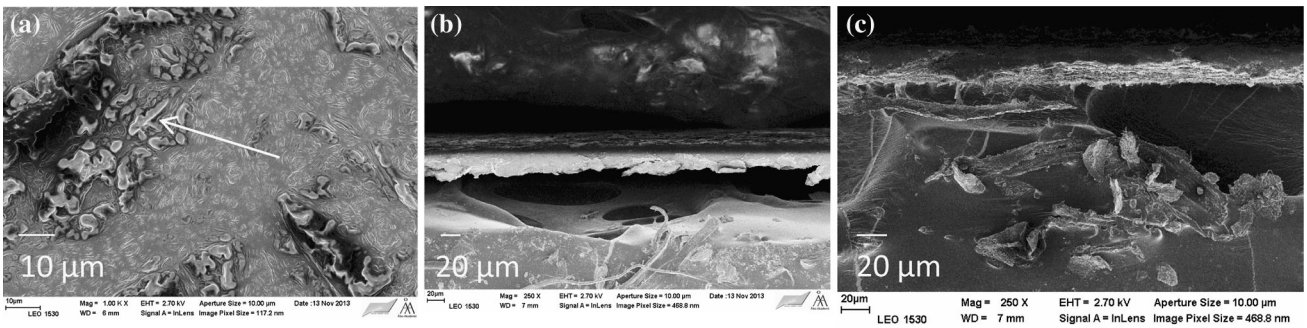

Fig. 5 SEM pictures of the possible oil deposition on a surface of NFC-film after 6 days exposure at 50 °C and at 50 % RH as picture (**a**) and as a cross-section, where the surface has turned to dark (**b**), and a cross-section without the oil exposure (**c**)

Su2 and GGM-Su1 coating on NFC-GGM films decreased OP values only moderately. GGM coating on pristine NFC film decreases OP slightly from 0.9 to 0.4 [(cm^3 µm)(m^2 kPa d)], GGM may have had better affinity onto NFC-GGM than GGM-Su and hence made a stronger barrier. However, the double-coating with GGM-Su2 gave the highest oxygen barrier with the excellent value of 0.1 [(cm^3 µm)(m^2 kPa d)] but the standard deviation was high, 0.2. Hydrogen bonding and Van der Waals forces of the films have been that strong, that the movement of fibrils were hindered. Further, the amorphous GGM-Su2 formed solid double-coating by filling up the porous surface of semi-crystalline NFC with good adhesion, thus preventing oxygen permeation. Thus with the modest 5.4 or 10.8 % weight increase of the film by the coating, the major enhancement in oxygen barrier can be achieved.

In another study by Stevanic et al. [24], arabinoxylans and GGM were reported to fill the voids of the NFC composite film and had OP values of 1.2–1.7 [(cm^3 µm)(m^2 kPa d)], while the pristine NFC films had the values of 2.5 [(cm^3 µm)(m^2 kPa d)]. This was the opposite of our case. Aulin, Gällstedt and Lindström, 2010 [42], recorded that the excellent grease and oxygen barrier properties of the carboxymethylated microfibrillated cellulose (CM-MFC) films are contributed by intra- and inter-fibrillar hydrogen bonding of semi-crystalline microfibrils. Another approach was to use the layer-by-layer deposition method alternating layers of (NFC) or carboxymethyl cellulose (CMC) with cationic polyethyleneimine (PEI) polyelectrolyte, on a flexible polylactic acid (PLA) substrate [43]. Hansen et al. [44] 2012 made 1:1 xylan-NFC films with various plasticisers. The presence of methoxypolyethylene glycol and glycerol decreased OP values of xylan-NFC films drastically. The OP value was 0.5 [(cm^3 µm)(m^2 kPa d)] for the CM-MFC and the PEI-CMC-PLA systems, 0.3 [(cm^3 µm)(m^2 kPa d)] for PEI-NFC-PLA system and 0.2 [(cm^3 µm)(m^2 kPa d)] for xylan-NFC films. Hot-pressed NFC films gave the values of 0.2 [(cm^3 µm)(m^2 kPa d)] [22]. The values are in a same range as our values. Pristine GGM films [45] and GGM-sorbitol films [38] showed values of 6.8 and 2.0 (cm^3 µm)(m^2 kPa d), respectively. With regard to other biopolymer films, the values of 150 and 160 [(cm^3 µm)(m^2 kPa d)] have been recorded for PLA and polyhydroxyalkanoate, respectively [46].

Dynamic mechanical analysis (DMA) in humidity mode

In good food packaging the material ought to withstand humidity alterations. We approached this by determining the stiffness. The storage moduli of NFC and the composite films after 300 min equilibration at 0, 50, 90 % and back to

Table 2 Oxygen permeability and transmission of the films

Film substrate	Coating	Film thickness	Oxygen permeability		Oxygen transmission	
		µm	[(cm^3 µm)(m^2 kPa d)]	Sd	cm^3/(m^2 d)	sd
NFC	–	35.5	0.5	0.07	1.4	0.2
NFC	GGM-Su2	32.5	0.3	0.00	0.9	0.03
NFC-GGM	–	28.0	0.9	0.04	3.2	0.2
NFC-GGM	GGM	35.5	0.4	0.03	1.1	0.1
NFC-GGM	GGM-Su1	37.5	0.8	0.01	2.1	0.2
NFC-GGM	GGM-Su2	43.4	0.6	0.04	1.4	0.08
NFC-GGM	GGM-Su2 X 2	49.5	0.1	0.2	0.2	0.3

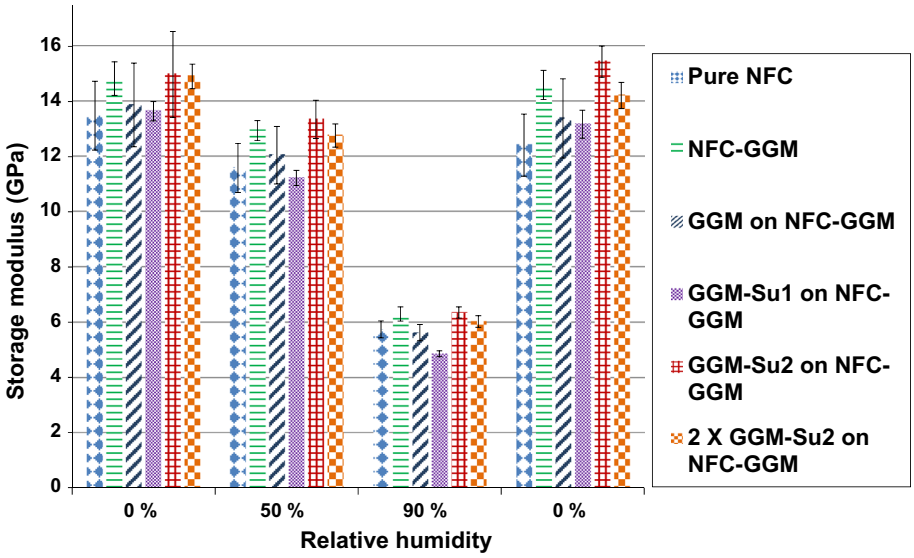

Fig. 6 The storage modulus with changing relative humidity of NFC, NFC-GGM, NFC-GGM coated with either GGM, GGM-Su1, GGM-Su2 or double coated with GGM-Su2

0 % RH are presented in Fig. 6. The storage moduli of the pristine NFC films and NFC-GGM films coated with GGM and GGM-Su2 exhibit fairly large standard deviations at 0 and 50 % RH, suggesting heterogeneous films with coatings. However, the average storage modulus values indicate trend-like differences between the films.

All films displayed similar behaviour with changing humidity levels: the highest moduli were observed after initial and final equilibration at 0 % RH. When the humidity was increased to 50 % RH, the moduli dropped slightly. Increasing the humidity further to 90 % RH caused a sharp drop in moduli. The deterioration of storage moduli with increasing humidity is attributed to water molecules diffusing into the film structure and disrupting the hydrogen bonding within and between the NFC fibrils and GGM. As a result, GGM chains are softened, hydrogen bonding between NFC fibrils weakened, and films plasticized. When the humidity was reduced back to 0 % RH, the moduli increased sharply, displaying recovery between 92 and 103 % relative to initial value at 0 % RH. The low moduli at high humidity and good recovery suggest slight irreversible slippage between the polymer chains and NFC fibrils within the films during exposure to humid conditions. However, the slippage is only partial and the interaction between the NFC network and the GGM preserves the film integrity well up to 50 % RH. The NFC-GGM with GGM-Su2 coating had clearly the highest recovery from 90 % back to 0 % RH, addressing the adhesion between GGM-Su2 and NFC.

The addition of GGM to NFC, as a coating of GGM-Su2 on NFC-GGM films, resulted in similar stiffer films. The stiffness followed a trend-like pattern at each humidity level and remained also at 90 % RH. We attribute the higher stiffness to GGM in the NFC-GGM films, since GGM readily adsorbs on cellulose fibrils in a rigid conformation [47]. Also high debranching of galactose contributed to higher sorption of GGM to NFC [24]. At relatively small amount (5.5 wt%), most of the GGM can adsorb directly on NFC fibrils without deteriorating the hydrogen-bonded network structure. At higher concentrations, GGM and other hemicelluloses are expected to reduce the stiffness of NFC films [48]. Adsorbed on NFC fibrils, GGM can potentially act as crosslinker/bridging agent for the NFC fibrils through hydrogen bonding, thus increasing the stiffness of NFC-GGM. GGM-Su2 on a film surface can potentially enhance stiffness via hydrogen bonding and via Van der Waals forces. GGM-Su2 was more hydrophobic than GGM-Su1 and GGM and hence contributed towards the higher stiffness on a film surface in moist conditions. Water possibly disrupts the hydrogen bonding network during coating, this may also favour stiffness of the GGM-Su2 coating, where ethanol was used as solvent. 25 wt% of arabionxylan with NFC decreased the storage modulus, but 15 wt% increase of hemicelluloses with NFC did not affect the storage modulus with increasing RH [24].

Concluding remarks

Succinic esters of GGM with two different DS values were synthesised (GGM-Su2 and GGM-Su1) and coated on the NFC reinforced composite films with 5.4 (single coating) or 10.8 wt% additions. The barrier properties and stiffness were improved by the addition of GGM-Su2 onto the NFC-GGM substrate. NFC-GGM composite films exhibited impenetrable grease barrier properties also at elevated temperatures. Very low OP value, 0.1 [(cm^3 μm)(m^2 kPa d)], was achieved with the GGM-Su2 double-coated NFC-GGM film. GGM-Su2 on GGM-NFC film and GGM within NFC network increased storage modulus at 0–90 %

RH. GGM can potentially act as a bridging agent for the NFC fibrils via hydrogen bonding. Pristine NFC, NFC-GGM and NFC-GGM films coated with GGM-Su2 exhibit moderate hydrophobic features according to the water CA dynamics on a film matrix interface. The level of hydrophobicity, oxygen barrier and stiffness of the film can be adjusted by the DS value of the hydrophobic moiety and by the architecture of the composites. The testing of the biodegradability of the biocomposites with added functional groups will be crucial in the next stage. This nanocellulose–hemicellulose based material has high potential as the grease and oxygen barrier for the dry item food packaging. There are environmental and economic motives to produce 100 % bio-based and quickly-enough-biodegradable material for the packaging. Plant-derived polysaccharides with added functionality may have a substantial role in this scenario.

Acknowledgements This work was carried out in framework of the Future Biorefinery Project by the Finnish Funding Agency for Technology and Innovation and Fibic Ltd. This work was part of the activities of the Åbo Akademi Process Chemistry Centre and Bioregs graduate school. This work made use of Aalto University Bioeconomy Facilities. We thank the staff of Metla in Vantaa and Lappeenranta University of Technology for providing the filtrated GGM, Hanna Lindqvist of our laboratory and Maristiina Nurmi of the Laboratory of Paper Coating and Converting for the practical help. The consultation on the concept by Lars Berglund of KTH, is highly appreciated.

References

1. Jayasiri HB, Purushothaman CS, Vennila A (2013) Quantitative analysis of plastic debris on recreational beaches in Mumbai, India. Mar Pollut Bull 77:107–112. doi:10.1016/j.marpolbul.2013.10.024
2. Thamae T, Bailie C (2008) Natural fibre composites, turning waste into useful materials. VDM Verlag Dr Muller Aktiengesellschaft & Co. Kg, pp 1–7
3. Willför S, Sjöholm R, Laine C et al (2003) Characterisation of water-soluble galactoglucomannans from Norway spruce wood and thermomechanical pulp. Carbohydr Polym 52:175–187
4. Song T, Pranovich A, Sumerskiy I, Holmbom B (2008) Extraction of galactoglucomannan from spruce wood with pressurised hot water. Holzforschung 62:659–666. doi:10.1515/HF.2008.131
5. Al Manasrah M, Kallioinen M, Ilvesniemi H, Maenttaeri M (2012) Recovery of galactoglucomannan from wood hydrolysate using regenerated cellulose ultrafiltration membranes. Bioresour Technol 114:375–381. doi:10.1016/j.biortech.2012.02.014
6. Rissanen JV, Grenman H, Xu C et al (2014) Obtaining spruce hemicelluloses of desired molar mass by using pressurized hot water extraction. ChemSusChem 7:2947–2953. doi:10.1002/cssc.201402282
7. Krogell J, Eranen K, Granholm K et al (2014) High-temperature pH measuring during hot-water extraction of hemicelluloses from wood. Ind Crop Prod 61:9–15. doi:10.1016/j.indcrop.2014.06.046
8. Kisonen V, Eklund P, Auer M et al (2012) Hydrophobication and characterisation of O-acetyl-galactoglucomannan for papermaking and barrier applications. Carbohydr Res 352:151–158. doi:10.1016/j.carres.2012.01.005
9. Mikkonen KS, Schmidt J, Vesterinen A-H, Tenkanen M (2013) Crosslinking with ammonium zirconium carbonate improves the formation and properties of spruce galactoglucomannan films. J Mater Sci 48:4205–4213. doi:10.1007/s10853-013-7233-9
10. Oinonen P, Areskogh D, Henriksson G (2013) Enzyme catalyzed cross-linking of spruce galactoglucomannan improves its applicability in barrier films. Carbohydr Polym 95:690–696. doi:10.1016/j.carbpol.2013.03.016
11. Kisonen V, Xu C, Eklund P et al (2014) Cationised O-acetyl galactoglucomannans: synthesis and characterisation. Carbohydr Polym 99:755–764. doi:10.1016/j.carbpol.2013.09.009
12. Lozhechnikova A, Dax D, Vartiainen J et al (2014) Modification of nanofibrillated cellulose using amphiphilic block-structured galactoglucomannans. Carbohydr Polym 110:163–172. doi:10.1016/j.carbpol.2014.03.087
13. Dax D, Eklund P, Hemming J et al (2013) Amphiphilic spruce galactoglucomannan derivatives based on naturally-occurring fatty acids. BioResources 8:3771–3790. doi:10.15376/biores.8.3.3771-3790
14. Mikkonen KS, Stevanic JS, Joly C et al (2011) Composite films from spruce galactoglucomannans with microfibrillated spruce wood cellulose. Cellulose 18:713–726. doi:10.1007/s10570-011-9524-0
15. Trovatti E, Fernandes SCM, Rubatat L et al (2012) Pullulan–nanofibrillated cellulose composite films with improved thermal and mechanical properties. Compos Sci Technol 72:1556–1561. doi:10.1016/j.compscitech.2012.06.003
16. Syverud K, Stenius P (2009) Strength and barrier properties of MFC films. Cellulose 16:75–85. doi:10.1007/s10570-008-9244-2
17. Besbes I, Vilar MR, Boufi S (2011) Nanofibrillated cellulose from alfa, eucalyptus and pine fibres: preparation, characteristics and reinforcing potential. Carbohydr Polym 86:1198–1206. doi:10.1016/j.carbpol.2011.06.015
18. Okuba K, Fujii T, Yamashita N (2005) Improvement of interfacial adhesion in bamboo polymer composite enhanced with micro-fibrillated cellulose. JSME Int J Ser Solid Mech Mater Eng 48:199–204
19. Zhang Z, Sèbe G, Rentsch D et al (2014) Ultralightweight and flexible silylated nanocellulose sponges for the selective removal of oil from water. Chem Mater 26:2659–2668. doi:10.1021/cm5004164
20. Xhanari K, Syverud K, Chinga-Carrasco G et al (2011) Structure of nanofibrillated cellulose layers at the o/w interface. J Colloid Interface Sci 356:58–62. doi:10.1016/j.jcis.2010.12.083
21. Vuoti S, Talja R, Johansson L-S et al (2013) Solvent impact on esterification and film formation ability of nanofibrillated cellulose. Cellulose 20:2359–2370. doi:10.1007/s10570-013-9983-6
22. Österberg M, Vartiainen J, Lucenius J et al (2013) A fast method to produce strong NFC films as a platform for barrier and functional materials. ACS Appl Mater Interfaces 5:4640–4647. doi:10.1021/am401046x
23. Zhou Q, Greffe L, Baumann MJ et al (2005) Use of xyloglucan as a molecular anchor for the elaboration of polymers from cellulose surfaces: a general route for the design of biocomposites. Macromolecules 38:3547–3549. doi:10.1021/ma047712k
24. Stevanic JS, Mikkonen KS, Xu C et al (2014) Wood cell wall mimicking for composite films of spruce nanofibrillated cellulose with spruce galactoglucomannan and arabinoglucuronoxylan. J Mater Sci 49:5043–5055. doi:10.1007/s10853-014-8210-7
25. Escalante A, Gonçalves A, Bodin A et al (2012) Flexible oxygen barrier films from spruce xylan. Carbohydr Polym 87:2381–2387. doi:10.1016/j.carbpol.2011.11.003
26. Isogai A (2013) Wood nanocelluloses: fundamentals and applications as new bio-based nanomaterials. J Wood Sci 59:449–459. doi:10.1007/s10086-013-1365-z

27. Henriksson M, Henriksson G, Berglund LA, Lindström T (2007) An environmentally friendly method for enzyme-assisted preparation of microfibrillated cellulose (MFC) nanofibers. Eur Polym J 43:3434–3441. doi:10.1016/j.eurpolymj.2007.05.038
28. Henriksson M, Berglund LA, Isaksson P et al (2008) Cellulose nanopaper structures of high toughness. Biomacromolecules 9:1579–1585. doi:10.1021/bm800038n
29. Sehaqui H, Zhou Q, Ikkala O, Berglund LA (2011) Strong and tough cellulose nanopaper with high specific surface area and porosity. Biomacromolecules 12:3638–3644. doi:10.1021/bm2008907
30. T 454 om-94 Turperntine test for voids in glassine and greaseproof papers (2000)
31. Bollstrom R, Saarinen JJ, Raty J, Toivakka M (2012) Measuring solvent barrier properties of paper. Meas Sci Technol 23:015601. doi:10.1088/0957-0233/23/1/015601
32. Kisonen V, Xu C, Bollström R et al (2014) O-acetyl galactoglucomannan esters for barrier coatings. Cellulose 21: 4497–4509. doi:10.1007/s10570-014-0428-7
33. Hannuksela T, Hervé du Penhoat C (2004) NMR structural determination of dissolved O-acetylated galactoglucomannan isolated from spruce thermomechanical pulp. Carbohydr Res 339:301–312. doi:10.1016/j.carres.2003.10.025
34. Ekholm FS, Ardá A, Eklund P et al (2012) Studies related to Norway spruce galactoglucomannans: chemical synthesis, conformation analysis, NMR spectroscopic characterization, and molecular recognition of model compounds. Chemistry 18:14392–14405. doi:10.1002/chem.201200510
35. Yuan Y, Lee TR (2013) Contact angle and wetting properties. In: Bracco G, Holst B (eds) Surface science techniques. Springer, Berlin, Heidelberg, pp 3–34
36. Spiridon I, Teacă C-A, Bodîrlău R, Bercea M (2013) Behavior of cellulose reinforced cross-linked starch composite films made with tartaric acid modified starch microparticles. J Polym Environ 21:431–440. doi:10.1007/s10924-012-0498-2
37. Kwak S-Y, Jung SG, Kim SH (2001) Structure-motion-performance relationship of flux-enhanced reverse osmosis (RO) membranes composed of aromatic polyamide thin films. Environ Sci Technol 35:4334–4340. doi:10.1021/es010630g
38. Hartman J, Albertsson A-C, Sjöberg J (2006) Surface- and bulk-modified galactoglucomannan hemicellulose films and film laminates for versatile oxygen barriers. Biomacromolecules 7:1983–1989. doi:10.1021/bm060129m
39. Kjellgren H, Gaellstedt M, Engstroem G, Jaernstroem L (2006) Barrier and surface properties of chitosan-coated greaseproof paper. Carbohydr Polym 65:453–460. doi:10.1016/j.carbpol.2006.02.005
40. Mikkonen KS, Heikkinen S, Soovre A et al (2009) Films from oat spelt arabinoxylan plasticized with glycerol and sorbitol. J Appl Polym Sci 114:457–466. doi:10.1002/app.30513
41. Kisonen V, Xu C, Böllstrom R et al (2014) O-acetyl galactoglucomannan esters for barrier coatings. Cellul Dordr Neth 21:4497–4509. doi:10.1007/s10570-014-0428-7
42. Aulin C, Gällstedt M, Lindström T (2010) Oxygen and oil barrier properties of microfibrillated cellulose films and coatings. Cellulose 17:559–574. doi:10.1007/s10570-009-9393-y
43. Aulin C, Karabulut E, Tran A et al (2013) Transparent nanocellulosic multilayer thin films on polylactic acid with tunable gas barrier properties. ACS Appl Mater Interfaces 5:7352–7359. doi:10.1021/am401700n
44. Hansen NML, Blomfeldt TOJ, Hedenqvist MS, Plackett DV (2012) Properties of plasticized composite films prepared from nanofibrillated cellulose and birch wood xylan. Cellul Dordr Neth 19:2015–2031. doi:10.1007/s10570-012-9764-7
45. Mikkonen KS, Tenkanen M (2012) Sustainable food-packaging materials based on future biorefinery products: xylans and mannans. Trends Food Sci Technol 28:90–102. doi:10.1016/j.tifs.2012.06.012
46. Van Tuil R, Fowler P, Lawther M, Weber CJ (2000) Properties of biobased packaging materials. In Biobased packaging materials for the food industry—Status and perspectives. KVL, Frederiksberg, pp 8–33
47. Eronen P, Österberg M, Heikkinen S et al (2011) Interactions of structurally different hemicelluloses with nanofibrillar cellulose. Carbohydr Polym 86:1281–1290. doi:10.1016/j.carbpol.2011.06.031
48. Hansen NML, Plackett D (2008) Sustainable films and coatings from hemicelluloses: a review. Biomacromolecules 9:1493–1505. doi:10.1021/bm800053z